

# Synthesis of Nanosilica from Sugarcane Bagasse Using the Sol-Gel Method for Enhanced Nano fluid Applications

Kagren John Kumar, Fuzieah Subari\*, Zalizawati Abdullah,  
Nor Hazelah Kasmuri, Nadia Kamaruddin

<sup>1</sup>*School of Chemical Engineering, College of Engineering,  
Universiti Teknologi MARA, 40450 Shah Alam, Selangor, Malaysia*

\*Corresponding Author's E-mail: [fuzieahsubari@uitm.edu.my](mailto:fuzieahsubari@uitm.edu.my)

Received: 11 September 2024

Accepted: 3 October 2024

Online First: 25 January 2025

## ABSTRACT

*Nanomaterials have gained immense popularity in advanced materials research due to their unique properties and potential applications in various fields. This study synthesizes nanofluids from ash-derived sugarcane bagasse nanosilica and evaluates their potential for practical and industrial applications. Using a sol-gel method and a two-step ultrasonication process, the nanofluids were characterized for particle size, agglomeration, stability, and viscosity. SEM images revealed irregularly shaped nanosilica particles with rough surfaces, indicating high surface areas and a tendency to agglomerate. UV-Vis spectroscopy showed that absorbance values decreased over time, indicating particle sedimentation or aggregation, with lower concentrations (0.05 wt.% and 0.10 wt.%) demonstrating better stability. Zeta potential measurements confirmed higher stability at lower concentrations due to stronger electrostatic repulsion, while viscosity measurements indicated effective dispersion without excessive thickening. Additionally, pH measurements revealed its critical role in maintaining the stability and dispersion of nanofluids, with optimal pH levels contributing to improved electrostatic interactions and reduced agglomeration. These findings suggest that lower concentrations of nanosilica provide better stability and dispersion in nanofluids, offering valuable insights for future formulation and application strategies in various industries.*

*Keywords: Nanosilica; Nanofluids; Biomass; Sol-gel; Sugarcane Bagasse*



Copyright© 2020 UiTM Press.  
This is an open access article  
under the CC BY-NC-ND license

## INTRODUCTION

Nanomaterials have emerged at the forefront of advanced materials research, offering unique size-dependent properties spanning optical, electrical, thermal, and mechanical domains. As the fundamental building blocks underpinning nanotechnology revolution, nanomaterials are poised to transform everything from biomedicine to energy systems [1]. Such biogenic nanofluids could replace conventional heat transfer fluids in applications ranging from electronics cooling to industrial heat exchangers. Their economic viability hinges on addressing scalability and dispersion stability limitations. Overall, nanofluid development from agricultural residues promotes sustainable nanomanufacturing while tackling biomass underutilization. This review focuses on two nanomaterials gradually gaining prominence which are nanosilica and nanofluids. Nanosilica refers to silicon dioxide particles fabricated at the nanoscale, exhibiting characteristics distinct from bulk silica [2]. Nanofluids describe engineered colloids comprising a base fluid with suspended nanoscale particles [3].

Nanosilica and nanofluids are two fascinating areas of research that have garnered significant attention due to their unique properties and potential applications. Nanosilica, referring to silica particles synthesized at the nanometer scale, exhibits size-dependent properties that make it suitable for reinforcing plastics, composite materials, and various industries such as construction, biomedicine, automotive, and aerospace [4]. However, challenges in terms of stability and dispersion of nanosilica in nanofluids and foam formation concerns hinder its full utilization. Nanofluids, which are suspensions of nanoparticles in a base fluid, have attracted attention for their potential applications. Nanosilica has unique properties that make it an attractive nanomaterial for various industries. However, achieving stability and dispersion of nanosilica in nanofluids presents challenges due to strong particle-particle forces [5].

One significant challenge when using nanosilica is foam formation, especially in industries like concrete and cement-based materials. Excessive foaming caused by nanosilica can impact the workability and stability of fresh concrete. However, careful dosage optimization of nanosilica can improve foam bubble stability while maintaining desired rheological properties [6]. Nanosilica can induce foam formation in water or humid

environments, affecting the performance of products in industries where it is used as a reinforcing agent or filler. This occurs due to the presence of water molecules on the surface of nanosilica particles, leading to hydrogen bonding and subsequent foam formation [7]. Several factors can affect the stability of nanosilica in nanofluids, including particle size, surface charge, and the surrounding medium's pH and viscosity [8]. Other variables, such as pH, temperature, and ionic strength, also play a significant role in nanosilica stability in nanofluids [9].

Recent progress in synthesizing nanosilica using both commodity chemicals and agricultural waste underscores its versatility and potential for sustainable production. Traditional synthesis methods such as sol-gel processing and carbon-thermal reduction have been extensively utilized [2]. However, the biogenic synthesis of nanosilica, which employs agricultural waste materials, presents an eco-friendly alternative that aligns with waste reduction and resource efficiency goals. Studies by Li *et al.* [1] and Prakash *et al.* [3] have highlighted the significant thermal conductivity improvements in nanofluids when nanosilica is utilized. Despite these findings, a gap remains in the literature comparing various biogenic synthesis techniques and their efficacy. Nanofluids, on the other hand, are liquid suspensions consisting of nanometer-sized particles dispersed in a base fluid. These fluids demonstrate enhanced heat transfer properties, particularly in terms of thermal conductivity [4]. This characteristic has led to their utilization in industries like automotive cooling, electronics cooling, solar energy systems, and heat exchangers.

Recent literature unraveling the novel properties and burgeoning applications for these nanomaterials, in addition to synthesizing diverse production pathways. Notably, nanosilica adoption continues rising in sectors like polymer composites, biomedicine, and catalysis. Its tunable morphology, ease of surface functionalization, and lack of toxicity underpins such widespread utility [2]. Nanosilica synthesis routes can utilize commodity chemicals or agricultural waste feedstocks via procedures like sol-gel processing or carbon-thermal reduction [10]. Alternatively, nanofluids boost heat transfer and thermal conductivity by leveraging conductivity enhancements at particle-fluid interfaces. This stimulates applications from solar thermal systems to electronic cooling [11]. Intriguingly, nanofluid properties depend on parameters including

particle material, size distribution, base fluid selection and temperature [12]. Promising one-step and two-step manufacturing pathways are compared.

## METHODOLOGY

### Material

Sugarcane bagasse, 10 ml of HCl 1 M, distilled water, 8 mL of 1 M NaOH and Chinese ink.

### Preparation of Nanosilica

The sugarcane bagasse was chopped into smaller pieces after being cleaned and dried. Sugarcane bagasse was calcined for two hours at 650°C. HCl 1 M were used to leach sugarcane bagasse ash by the ratio 10;1 (HCl: ash). Then, the mixture was continuously agitated for one hour at 100°C. The residue underwent several washes with distilled water after the leached sugarcane bagasse ash mixture was being filtered. 1 M NaOH was added to the washed residue in the ratio of 8:1 (NaOH: residue). The mixture then was continuously agitated for one hour at 100°C. Sodium silicate was the filtrate obtained from the filtered mixture. For the gelling procedure, the solution was titrated with 1 M HCl until pH 7 was achieved. The aqua gel was created. It was oven for 1 hour at 60°C. The powdered xerogel made of synthetic silica that was ground in an agate mortar. To produce silica nanoparticles of uniform size, the resulting silica nanoparticles were sorted using a 200-mesh screen.

### Two-step method of Nanofluid

In this method, nanosilica was firstly prepared by using sol-gel method. The nanosilica produced with a concentration ranging from 0.05–0.20 wt.% were added into Chinese ink-distilled water solution to produce nanofluids using two-step as depicted in Figure 1. Chinese ink as shown in Figure 2 was used as surfactant because carbon black particles and animal glue which is collagen are presented in the Chinese ink [13]. This allow Chinese ink functioning as an effective surfactant to improve nanoparticles stability in

base fluid. The distilled water acts as the base fluid of the suspension. Then, the nanofluid was dispersed using ultrasonic bath (Elmasonic S 80 H) for 20 minutes to break down the agglomeration of nanoparticles.

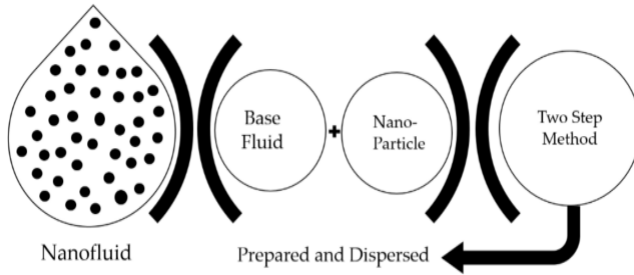


Figure 1: Illustration of two-step method [14]



(a)



(b)

Figure 2: (a) Chinese ink (b) Chinese ink-distilled water solution

## Characterization of Nanosilica

The raw and modified clinoptilolite functional groups were examined using a Fourier transform infrared spectrophotometer (PERKIN ELMER, United States). The infrared spectra were recorded with a scanning frequency ranging from 515 to 4000  $\text{cm}^{-1}$ . The morphology of nanosilica powder synthesized from sugarcane bagasse was examined using scanning electron microscopy (SU3500, 2021, Japan) at magnifications of 5000X, 10,000X, and 15,000X. The voltage applied for SEM image analysis is 15 kilovolts (kV). The SEM images were captured to analyze the morphology, size distribution of aggregates, porosity, and texture of the particles.

## **Characterization of Nanofluid**

### **Zetasizer Nano (ZSN)**

Zetasizer Nano (MPT-2, 2019, United Kingdom) was employed for the analysis of the nanofluid composed of nanosilica synthesized from sugarcane bagasse and dispersed in a Chinese ink-distilled water solution. The nanofluid was loaded into a disposable polystyrene cuvette designed to facilitate accurate measurements. The Zetasizer Nano uses dynamic light scattering (DLS) to determine the particle size distribution by analyzing the fluctuations in light intensity caused by the Brownian motion of the particles. Additionally, electrophoretic light scattering (ELS) was utilized to measure the zeta potential, which indicates the surface charge and stability of the nanofluid.

### **Ultraviolet–visible spectroscopy (Uv-vis)**

UV-vis spectroscopy (Spectrophotometer DR 2700) was employed to analyze the optical properties of a nanofluid composed of nanosilica synthesized from sugarcane bagasse and dispersed in a Chinese ink-distilled water solution. The procedure involves filling a clean cuvette with the nanofluid and placing it in a UV-Vis spectrophotometer. The spectrophotometer measures the absorbance of light across the ultraviolet and visible spectrum, capturing the characteristic absorption peaks of both the nanosilica and the ink. These absorption spectra provide insights into the dispersion quality, particle interaction, and stability of the nanofluid, which are critical for assessing its suitability for various applications.

### **Vibro Viscometer**

The viscosity of the nanofluid, which includes nanosilica synthesized from sugarcane bagasse suspended in a Chinese ink-distilled water solution, was measured using a vibro viscometer (SV-10, Tokyo). The nanofluid sample was poured into the sample cup, ensuring it was free of air bubbles and impurities. The sensor plates of the viscometer were then immersed in the nanofluid, and the device was activated. The vibro viscometer measures viscosity by detecting the resistance against the oscillating motion of the sensor plates within the fluid. This provides a precise and rapid determination of the nanofluid's viscosity, which is essential for evaluating its flow properties and potential applications.

## pH Meter

The pH of the nanofluid, which comprises nanosilica synthesized from sugarcane bagasse and suspended in a Chinese ink-distilled water solution, was determined using a digital pH meter (Mettler Toledo pH meter F-20, China). The nanofluid sample was then placed in a clean beaker, and the pH electrode was immersed into the solution. The pH reading was allowed to stabilize before being recorded.

## RESULTS AND DISCUSSION

### Characterization of Nanosilica

In this study, nanosilica powder was successfully produced from sugarcane bagasse using the sol-gel method as shown in Figure 3. The process involved converting the bagasse into a silica-rich solution, which was then precipitated and processed into nanosilica, demonstrating an effective and sustainable approach to repurposing agricultural waste.

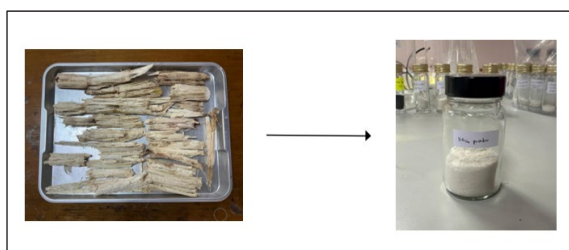
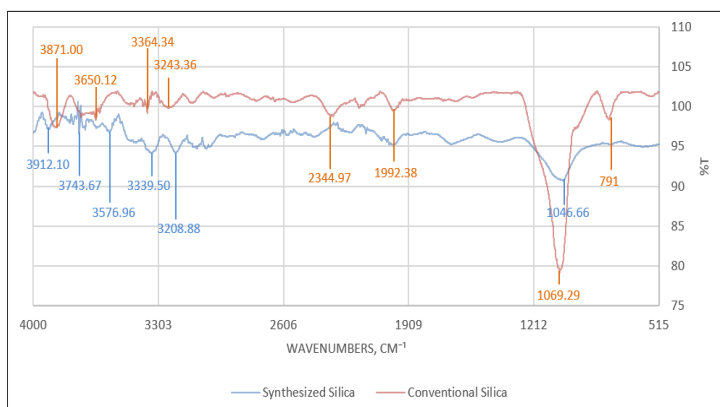


Figure 3: Sugarcane bagasse to nanosilica powder

### Fourier Transform Infrared Spectroscopy (FTIR)

The FTIR spectrum of conventional silica powder, presented in Figure 4 (Red line), serves as a benchmark for silica characterization. It exhibits characteristic peaks at wavenumbers  $3871\text{ cm}^{-1}$ ,  $3650\text{ cm}^{-1}$ ,  $3364\text{ cm}^{-1}$ , and  $3243\text{ cm}^{-1}$ , corresponding to O-H and N-H stretching vibrations. These peaks indicate the presence of hydroxyl and amine groups. The peak observed at  $2344\text{ cm}^{-1}$  is associated with C=O stretching vibrations, suggesting the presence of carbon dioxide. Additionally, significant peaks at  $1069\text{ cm}^{-1}$

and  $791\text{ cm}^{-1}$  are attributed to Si-O-Si stretching vibrations, confirming the silica structure [15].



**Figure 4: FTIR spectra comparing conventional and synthesized silica powders**

In contrast, the FTIR spectrum of synthesized silica powder, depicted in Figure 4 (Blue line), displays peaks at wavenumbers  $3912\text{ cm}^{-1}$ ,  $3743\text{ cm}^{-1}$ ,  $3576\text{ cm}^{-1}$ ,  $3339\text{ cm}^{-1}$ , and  $3208\text{ cm}^{-1}$ , corresponding to O-H and N-H stretching vibrations. These peaks are slightly shifted compared to those in the conventional silica spectrum, indicating possible differences in hydrogen bonding and surface hydroxyl groups. Notably, the pronounced peak at  $1046\text{ cm}^{-1}$ , attributed to Si-O-Si stretching, falls within the  $1000\text{--}1100\text{ cm}^{-1}$  range. The presence and intensity of this peak confirm the successful abstraction of silica from sugarcane bagasse.

The focus of this analysis is on the main Si-O-Si stretching vibration band which is at wavenumbers around  $1000\text{--}1100\text{ cm}^{-1}$  [16]. The significant peak at  $1046\text{ cm}^{-1}$  in the synthesized silica powder is a critical indicator of the successful extraction of silica from sugarcane bagasse. This peak's presence and intensity highlight the efficiency of the synthesis process, distinguishing the synthesized silica from the conventional benchmark.

## Morphological Characterization (SEM)

The scanning electron microscopy (SEM) images provide a detailed examination of the nanosilica particles at varying magnifications as shown



in Figure 5. At 1,000x magnification (Figure 5(a)), the particles exhibit an irregular and rough morphology with various sizes and shapes, forming visible agglomerates.

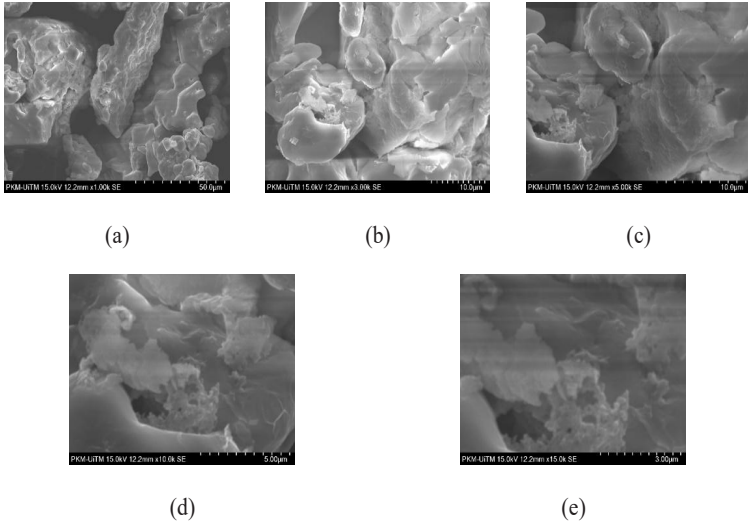


**Figure 5: SEM Images of Nanosilica at (a) 1000X Magnifications (b) 3000X Magnifications (c) 5000X Magnifications (d) 10000X Magnifications (e) 15000X Magnifications**

This rough texture suggests a high surface area, which is characteristic of nanosilica materials. Similar morphological characteristics have been observed in nanosilica synthesized from rice husk and wheat husk, where irregular shapes and rough surfaces were reported, indicating high surface areas suitable for various applications [17].

At 3,000x magnification (Figure 5(b)) reveals irregularly shaped particles with rough surfaces. These particles appear to cluster together, indicating potential agglomeration, which is typical for nanosilica due to the high surface energy of nanoparticles. The size distribution within this image is heterogeneous, with some particles forming larger aggregates possibly composed of smaller individual units. This behavior aligns with findings from other studies on nanosilica synthesized from biomass sources, such as rice husk and corn cob, where similar agglomeration and size distribution patterns were noted [17].

Increasing the magnification to 5,000x (Figure 5(c)) reveals finer structural details and porosity. The interconnected nature of smaller particles forming larger aggregates becomes more evident, highlighting the material's high surface energy and tendency for agglomeration. This magnification also accentuates the porosity of the nanosilica, with visible pore structures that enhance the material's surface area. These characteristics are critical for applications in catalysis and adsorption, where large surface areas and high reactivity are advantageous. These characteristics are critical for applications in catalysis and adsorption, as noted in studies involving nanosilica derived from rice husk and sugarcane bagasse [17].

Taken at a higher magnification of 10000x with a scale bar of 5.0  $\mu\text{m}$  (Figure 5(d)), the nanosilica particles' irregular shapes and surface details become more pronounced. This closer inspection highlights the roughness and irregularities of the surfaces, showcasing the high surface area characteristic of nanosilica. Additionally, some particles exhibit porous structures, enhancing their applicability in fields that require large surface areas, such as catalysis or adsorption. The visibility of pores at this scale underscores the potential for enhanced adsorption capacities, like those observed in nanosilica derived from other agricultural wastes like rice husk ash and corn cob residues [17].

At the highest magnification of 15,000x (Figure 5(e)), the intricate surface texture and presence of fine pores and channels are clearly visible. Individual nanostructures within the aggregates can be observed, providing insights into the nanoscale features of the silica particles, such as surface roughness and porosity. The fine porosity and extensive surface area observed at this level are indicative of the nanosilica's high potential for applications in fields such as environmental remediation, where large surface areas and reactive sites are essential. The nanosilica's high surface energy and fine structure at this magnification underline its potential in advanced applications, such as drug delivery systems, where precise interaction at the nano level is crucial [17].

## Analysis of Nanofluid

### Zetasizer Nano (ZSN)

In this study, we investigated the stability of nanofluids formulated with nanosilica synthesized from sugarcane bagasse and dispersed in a Chinese ink-distilled water solution. The stability of these nanofluids was assessed through zeta potential measurements as displayed in Figure 6, which reflect the electrostatic interactions within the colloidal suspension.

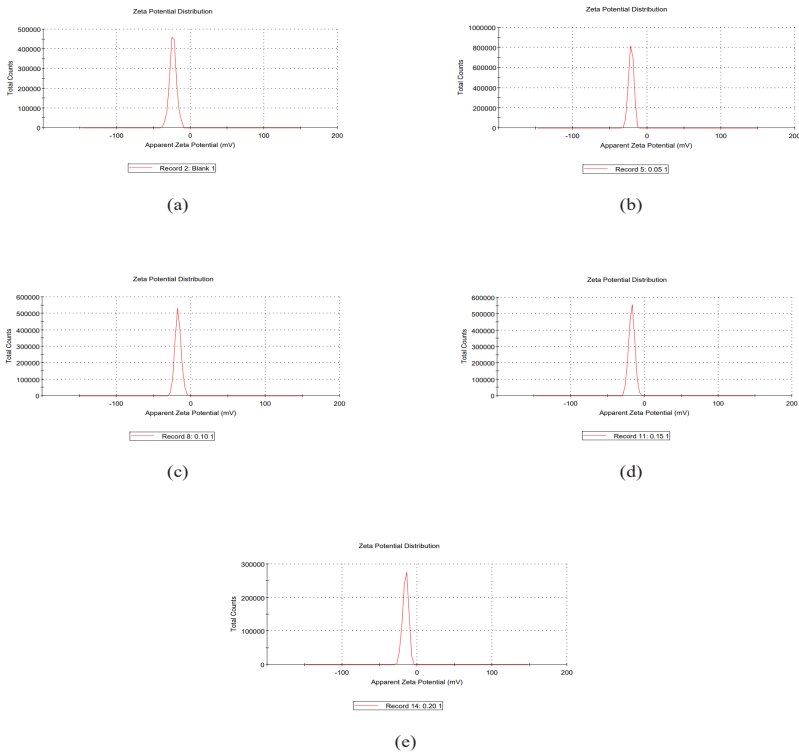


**Figure 6: Zeta potential graph for different nanosilica composition (a) blank (b) 0.05 wt.% (c) 0.10 wt.% (d) 0.15 wt.% (e) 0.20 wt.%**

The base fluid, comprising only the Chinese ink-distilled water solution without nanosilica, exhibited a zeta potential of  $-23.7$  mV (Figure 6 (a)), indicating strong electrostatic repulsion and high stability in the absence of nanoparticles. Upon introducing 0.05 wt.% nanosilica into the nanofluid, the zeta potential decreased to  $-21.4$  mV (Figure 6 (b)), suggesting a slight

reduction in electrostatic repulsion but still maintaining moderate stability with well-dispersed nanoparticles. Increasing the nanosilica concentration to 0.10 wt.% resulted in a further decrease in zeta potential to -17.5 mV (Figure 6 (c)), indicating a continued reduction in repulsive forces and potentially higher susceptibility to particle aggregation. Notably, at 0.15 wt.% nanosilica, the zeta potential decreased marginally to -17.6 mV (Figure 6 (d)), suggesting comparable stability to the 0.10 wt.% concentration despite the higher nanoparticle loading. However, at 0.20 wt.% nanosilica, the zeta potential decreased further to -15.5 mV (Figure 6 (e)), indicating a trend towards reduced stability with increased nanoparticle loading. These results suggest that while lower concentrations of nanosilica may offer better stability with higher zeta potentials, higher concentrations can lead to diminished stability due to reduced electrostatic repulsion and increased aggregation tendencies. Cruz Schneid *et. al* [18] investigated the behavior of silica nanoparticle suspensions and found that the zeta potential decreases with increasing nanoparticle concentration. This decrease in zeta potential leads to particle aggregation and reduced stability of the suspension. Metin *et.al* [19] emphasizes the importance of nanoparticle concentration in maintaining the stability of colloidal suspensions and highlights how higher concentrations can significantly affect the electrostatic interactions and overall dispersion stability. Further investigations into optimizing nanosilica concentrations and understanding the role of Chinese ink as a dispersant will be crucial for enhancing the stability of nanofluids in various practical applications.

### **Ultraviolet–visible spectroscopy (UV-vis)**

The stability of nanofluids formulated with nanosilica synthesized from sugarcane bagasse and dispersed in a Chinese ink-distilled water solution was investigated using UV-Vis spectroscopy as shown in Figure 7. Absorbance readings were recorded at various time intervals (0, 30, 60, 90, and 120 minutes) for different concentrations of nanosilica (0.05 wt.%, 0.10 wt.%, 0.15 wt.%, and 0.20 wt.%), along with a blank sample for comparison. From Figure 7, the initial absorbance values increased with the concentration of nanosilica, with the highest absorbance at 0 minutes observed for the 0.20 wt.% concentration (3.021) and the lowest for the blank sample (2.799), indicating a higher number of dispersed particles in the nanofluid at higher concentrations.

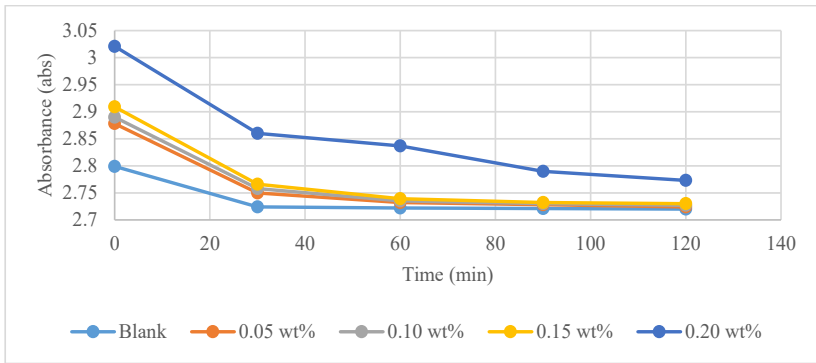


**Figure 7: Graph of absorbance reading for different concentrations against time**

Over time, absorbance values for all concentrations decreased, suggesting sedimentation or aggregation of nanosilica particles, which leads to a reduction in the number of dispersed particles in the solution. The most rapid decrease in absorbance occurred within the first 30 minutes, after which the values gradually stabilized. Among the different concentrations, the 0.20 wt.% concentration showed the most significant decrease in absorbance, indicating less stability compared to lower concentrations. In contrast, the 0.05 wt.% and 0.10 wt.% concentrations exhibited smaller changes in absorbance over time, suggesting better stability. At the 120-minute mark, absorbance values across all samples converged, with the 0.20 wt.% concentration still displaying the highest absorbance (2.773), though much reduced from the initial reading. The blank sample maintained the lowest absorbance throughout the experiment, as expected due to the absence of nanosilica particles. The UV-Vis analysis demonstrates that the stability of nanosilica-dispersed nanofluids varies with concentration. Based on the data obtained, these findings substantiate the conclusions of Pham and Nguyen [20] who observed that lower concentrations of nanosilica exhibit greater stability due to reduced inter-particle interactions, thereby mitigating the likelihood of aggregation and sedimentation. Their study highlights that higher concentrations lead to increased particle collisions, promoting aggregation and subsequent instability, resulting in a noticeable decline in absorbance over time.

Lower concentrations (0.05 wt.%, 0.10 wt.% and 0.15 wt.%) exhibit better stability over time, with smaller decreases in absorbance, indicating that the nanosilica particles remain more evenly dispersed. In contrast, higher concentrations (0.20 wt.%) show greater initial absorbance but experience more significant decreases, suggesting aggregation and sedimentation of particles. For applications requiring stable nanofluids, it may be advantageous to use lower concentrations of nanosilica to maintain a more stable dispersion over time. This analysis provides valuable insights into the behavior of nanosilica in nanofluids, which can inform future formulation and application strategies.

### **Viscosity of Nanofluid**

The viscosity of the nanofluid formulated with nanosilica synthesized from sugarcane bagasse and dispersed in a Chinese ink-distilled water solution was measured using a vibro viscometer. Figure 8 summarizes viscosity reading for different concentrations nanosilica in nanofluid. From Figure 8, the base fluid (0 wt.% nanosilica) exhibited a viscosity of 0.91 mPas. With the addition of 0.05 wt.% nanosilica, the viscosity increased slightly to 0.92 mPas. Further increments in nanosilica concentration to 0.10 wt.%, 0.15 wt.%, and 0.20 wt.% resulted in viscosities of 0.93 mPas, 0.94 mPas, and 0.95 mPas, respectively. These results indicate a gradual and consistent increase in viscosity with increasing nanosilica concentration. This trend suggests effective dispersion of the nanosilica particles within the base fluid, enhancing its resistance to flow without causing excessive thickening. The modest increase in viscosity, approximately 4.4% at the highest concentration, highlights the compatibility and potential of the sugarcane bagasse-derived nanosilica for nanofluid applications. This formulation provides a stable suspension with improved viscosity, suitable for applications requiring enhanced thermal properties while maintaining manageable fluidity.

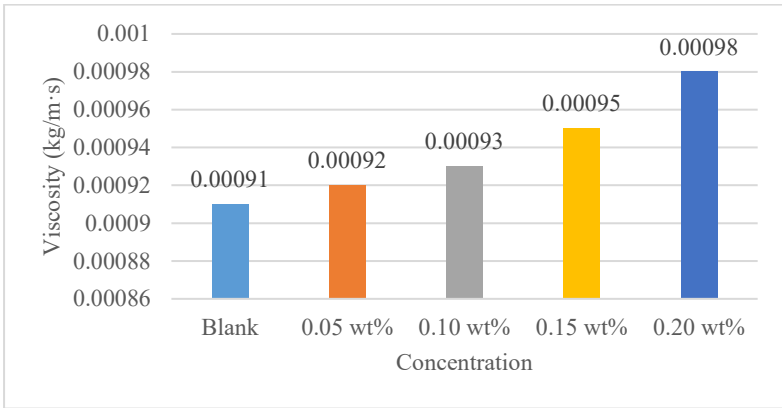


**Figure 8: Viscosity at different concentrations nanosilica in nanofluid**

The result aligns with the findings of previous research, which has consistently reported that higher nanoparticle concentrations lead to an increase in the viscosity of nanofluids [21]. The observed increase in viscosity with higher concentrations of nanosilica can be attributed to the enhanced interaction and aggregation of nanoparticles within the fluid. This behavior has been corroborated by several studies, wherein the viscosity of nanofluids was found to increase proportionally with nanoparticle concentration due to intensified particle-particle interactions [22]. These findings highlight the necessity to optimize nanoparticle concentrations in nanofluids to achieve a balance between enhanced thermal properties and manageable viscosity levels for practical applications.

### pH of Nanofluid

The results exhibit a distinct trend that as the concentration of nanosilica increases, the pH of the nanofluid transitions from acidic to basic. The pH value of nanosilica in nanofluid at concentration 0.05 wt.% to 0.2 wt.% is shown in Figure 9. The control sample devoid of nanosilica, presents a pH of 5.29 which indicates a slightly acidic environment. Introducing 0.05% nanosilica significantly elevates the pH to 8.46, indicating a shift to basic conditions. Further increments in nanosilica concentration continue to increase the pH values, with the highest tested concentration of 0.20% achieving a pH of 9.02. These findings suggest that nanosilica from

sugarcane bagasse has alkaline properties that significantly increase the pH of the nanofluid. This increase is likely due to the hydroxyl groups on the nanosilica particles, which release hydroxide ions (OH<sup>-</sup>) into the fluid. Similar studies support these results. For example, research on nanosilica from rice husk ash found that it increased the pH of water due to the release of hydroxide ions [23]. Nanosilica from wheat husk showed similar behavior, raising pH by interacting with water and releasing hydroxide ions [24]. Studies on nanosilica from corn cob also confirm this trend, with the particles increasing pH by introducing hydroxide ions into the solution [25].

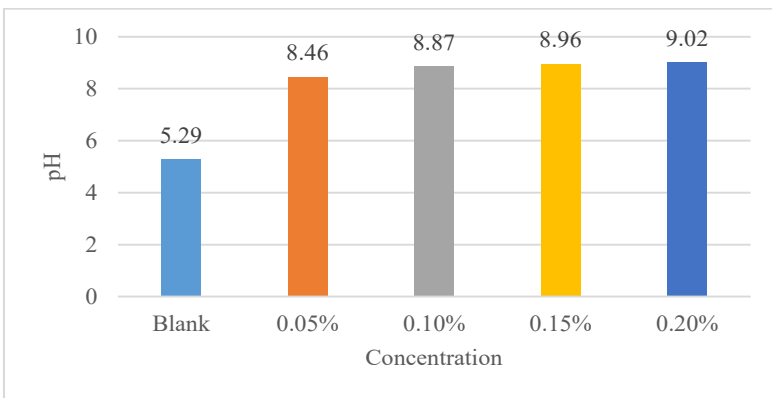


Figure 9: pH at different concentrations nanosilica in nanofluid

## CONCLUSION

This study examined the stability and properties of nanofluids made with nanosilica synthesized from sugarcane bagasse, dispersed in a Chinese ink-distilled water solution. The nanosilica particles were found to have irregular shapes and rough surfaces, typical of high surface area materials. They also showed a tendency to agglomerate due to their high surface energy. UV-Vis spectroscopy revealed that absorbance values decreased over time for all concentrations, indicating particle sedimentation or aggregation. Higher concentrations (0.20 wt.%) were less stable compared to lower concentrations (0.05 wt.% and 0.10 wt.%). Zeta potential measurements supported these findings, showing that lower concentrations had higher zeta potential values, indicating better stability due to stronger electrostatic



repulsion. Higher concentrations had lower zeta potential values, suggesting increased particle aggregation. Viscosity measurements showed a gradual increase with higher nanosilica concentrations, demonstrating effective nanoparticle dispersion within the base fluid without excessive thickening. The pH of the nanofluid increased as more nanosilica was added, starting from a slightly acidic pH of 5.29 without nanosilica to a basic pH of 9.02 at the highest concentration. This is due to the release of hydroxide ions (OH<sup>-</sup>) from the nanosilica particles. In summary, lower concentrations of nanosilica (0.05 wt.% and 0.10 wt.%) provided better stability and dispersion, making them more suitable for practical applications. The ability of nanosilica to change the pH of the nanofluid can be useful for applications that need specific pH levels. This study provides useful insights for improving the formulation and use of nanosilica in various industries.

## ACKNOWLEDGEMENT

The author would like to acknowledge Universiti Teknologi MARA. UiTM for providing support in completing this research study.

## REFERENCES

- [1] J. Li, X. Zhang, B. Xu, & M. Yuan, 2021. Nanofluid Research and Applications: A Review, *International Communications in Heat and Mass Transfer*, 127, 105543.
- [2] P. Singh, S. Srivastava, & S. K. Singh, 2019. Nanosilica: Recent Progress in Synthesis, Functionalization, Biocompatibility, and Biomedical Applications, *ACS Biomaterials Science & Engineering*, 5(10), 4882-4898.
- [3] S. B. Prakash, K. N. Kotin, & P. Kumar, 2020. Preparation and Characterization of Nanofluid (CuO–water, TiO<sub>2</sub>–water), *EPH-International Journal of Science and Engineering*, 6(3), 13-18.
- [4] H. Zamani, A. Jafari, S. M. Mousavi, & E. Darezereshki, 2020. Biosynthesis of Silica Nanoparticle using *Saccharomyces Cerevisiae*

- and Its Application on Enhanced Oil Recovery, *Journal of Petroleum Science and Engineering*, 190, 107002.
- [5] Z. Zhe, & A. Yuxiu, 2018. Nanotechnology for The Oil and Gas Industry—An Overview of Recent Progress, *Nanotechnology Reviews*, 7(4), 341-353.
- [6] M. Abd Elrahman, P. Sikora, S. Y. Chung, & D. Stephan, 2021. The Performance of Ultra-Lightweight Foamed Concrete Incorporating Nanosilica, *Archives of Civil and Mechanical Engineering*, 21(2), 79.
- [7] Z. Briceño-Ahumada, J. F. A. Soltero-Martínez & R. Castillo, 2021. Aqueous Foams and Emulsions Stabilized by Mixtures of Silica Nanoparticles and Surfactants: A State-Of-The-Art Review, *Chemical Engineering Journal Advances*, 7, 100116.
- [8] M. J. Lourenço, J. Alexandre, C. Huisman, X. Paredes, & C. Nieto de Castro, 2021. The Balance Between Energy, Environmental Security, and Technical Performance: The Regulatory Challenge of Nanofluids, *Nanomaterials*, 11(8), 1871.
- [9] M. Adil, H. Mohd Zaid, F. Raza, & M. A. Agam, 2020. Experimental Evaluation of Oil Recovery Mechanism Using a Variety of Surface-modified Silica Nanoparticles: Role of In-situ Surface-modification in Oil-wet System, *Plos One*, 15(7), e0236837.
- [10] N. S. Seroka, R. T. Taziwa, & L. Khotseng, 2022. Extraction and Synthesis of Silicon Nanoparticles (SiNPs) from Sugarcane Bagasse Ash: A Mini-review, *Applied Sciences*, 12(5), 2310.
- [11] G. F. Smaism, D. B. Mohammed, A. M. Abdulhadi, K. F. Uktamov, F. H. Alsultany, S. E. Izzat, & E. Kianfar, 2022. Retracted Article: Nanofluids: Properties and Applications, *Journal of Sol-Gel Science and Technology*, 104(1), 1-35.
- [12] S. Kalsi, S. Kumar, A. Kumar, T. Alam, & D. Dobrotă, 2023. Thermophysical Properties of Nanofluids and Their Potential Applications in Heat Transfer Enhancement: A Review, *Arabian*

*Journal of Chemistry*, 105272.

- [13] H. Wang, W. Yang, L. Cheng, C. Guan, & H. Yan, 2018. Chinese Ink: High Performance Nanofluids for Solar Energy, *Solar Energy Materials and Solar Cells*, 176, 374-380.
- [14] H. M. Ali, H. Babar, T. R. Shah, M. U. Sajid, M. A. Qasim, & S. Javed, 2018. Preparation Techniques of TiO<sub>2</sub> Nanofluids and Challenges: A Review, *Applied Sciences*, 8(4), 587.
- [15] P. Chindapasirt, & U. Rattanasak, 2020. Eco-production of Silica from Sugarcane Bagasse Ash for Use as a Photochromic Pigment Filler, *Scientific Reports*, 10(1), 9890.
- [16] B. Yan, S. Liu, M. L. Chastain, S. Yang, & J. Chen, 2021. A New FTIR Method for Estimating the Firing Temperature of Ceramic Bronze-casting Moulds from Early China, *Scientific Reports*, 11(1), 3316.
- [17] W. Guo, G. Li, Y. Zheng, & K. Li, 2021. Nano-silica Extracted from Rice Husk and Its Application in Acetic Acid Steam Reforming, *RSC Advances*, 11(55), 34915-34922.
- [18] A. da Cruz Schneid, L. J. C. Albuquerque, G. B. Mondo, M. Ceolin, A. S. Picco, & M. B. Cardoso, 2022. Colloidal Stability and Degradability of Silica Nanoparticles in Biological Fluids: A Review, *Journal of Sol-Gel Science and Technology*, 102(1), 41-62.
- [19] C. O. Metin, L. W. Lake, C. R. Miranda, & Q. P. Nguyen, 2011. Stability of Aqueous Silica Nanoparticle Dispersions, *Journal of Nanoparticle Research*, 13, 839-850.
- [20] H. Pham, & Q. P. Nguyen, 2014. Effect of Silica Nanoparticles on Clay Swelling and Aqueous Stability of Nanoparticle Dispersions, *Journal of Nanoparticle Research*, 16, 1-11.
- [21] S. M. S. Murshed, K. C. Leong, & C. Yang, 2008. Investigations of Thermal Conductivity and Viscosity of Nanofluids, *International*

*Journal of Thermal Sciences*, 47(5), 560-568.

- [22] R. Sadeghi, S. G. Etemad, E. Keshavarzi, & M. Haghshenasfard, 2015. Investigation of Alumina Nanofluid Stability by UV–vis Spectrum, *Microfluidics and Nanofluidics*, 18, 1023-1030.
- [23] D. Datta, & G. Halder, 2019. Effect of Rice Husk Derived Nanosilica on the Structure, Properties and Biodegradability of Corn-starch/LDPE Composites, *Journal of Polymers and the Environment*, 27, 710-727.
- [24] F. Akhter, A. R. Jamali, M. N. Abbasi, M. A. Mallah, A. A. Rao, S. A. Wahocho, & Z. A. Chandio, 2023. A Comprehensive Review of Hydrophobic Silica and Composite Aerogels: Synthesis, Properties and Recent Progress Towards Environmental Remediation and Biomedical Applications, *Environmental Science and Pollution Research*, 30(5), 11226-1124.
- [25] S. Prabha, D. Durgalakshmi, S. Rajendran, & E. Lichtfouse, 2021. Plant-derived Silica Nanoparticles and Composites for Biosensors, Bioimaging, Drug Delivery and Supercapacitors: *A Review*, *Environmental Chemistry Letters*, 19(2), 1667-1691.